JOURNAL OF CATALYSIS 58, 361–369 (1979)

Mössbauer Investigation of Supported Fe Catalysts

III. *In Situ* Kinetics and Spectroscopy during Fischer–Tropsch Synthesis

G. B. RAUPP[1] AND W. N. DELGASS

School of Chemical Engineering, Purdue University, West Lafayette, Indiana 47907

Received July 13, 1978; revised January 9, 1979

In situ constant velocity Mössbauer data have been used to measure the rate of carbiding of 10Fe/SiO_2 and 10Fe/MgO during the Fischer–Tropsch synthesis reaction at 523°K and 3.3 H_2/CO. Simultaneous spectroscopic and kinetic measurements reveal the remarkable result that the reaction rate follows the extent of bulk carbide formation and, thus, that incorporation of carbon into the iron particles controls the number of active surface sites until carbiding is complete. Conversion, paraffin to olefin ratio, and C_2/C_1 ratio increase with extent of carbiding. Hydrogenation of a fully carbided catalyst at 523°K is slow and produces only methane.

INTRODUCTION

In the ideal spectroscopic experiment in catalysis, one would examine the surface chemistry of a "real" catalyst *in situ* at reaction conditions. Unfortunately, many popular spectroscopic techniques have inherent limitations, such as requirements of ultra-high vacuum (UHV) or that the catalyst be in the form of a single crystal or metal foil, that prohibit this ideal experiment. Mössbauer effect measurements, however, offer specific advantages for *in situ* application. Incident γ-rays in the keV range have negligible interaction with reacting gases. The relatively high penetrating power of the γ-rays also means that atoms deep within pores of a support are "seen" as easily as those on the exterior of the support particle. Furthermore, when the active metal is well dispersed on the support, a large fraction of the resonant atoms are surface atoms and thus the Mössbauer effect can, in fact, sample surface chemistry. Typical accumulation times for Mössbauer spectra of 1–10 wt% Fe samples taken with a 50-mCi source are 4–6 hr. One way to speed the experiment to see important changes which occur in as little as a few minutes of reaction time is to concentrate the full γ-ray intensity of the source in a narrow energy region where major spectral changes occur. Such data can be collected readily on a Mössbauer spectrometer equipped with a constant velocity drive signal.

In previous work in this series we have examined the effects of pretreatment on Fe particle size (*1*) and the role of support, particle size, and alloying on the formation of iron carbide during the Fischer–Tropsch synthesis reaction (*2*). The latter study showed that the carbide phase formed (ϵ', ϵ, or χ) at 523°K depends on the nature of the catalyst, and that at steady state, all the iron which can be reduced in H_2 to the metal in Fe/SiO_2 and Fe/MgO catalysts is carbided during reaction.

[1] Present address: Exxon Research & Engineering Company, Florham Park, N. J. 07932.

0021-9517/79/090361-09$02.00/0

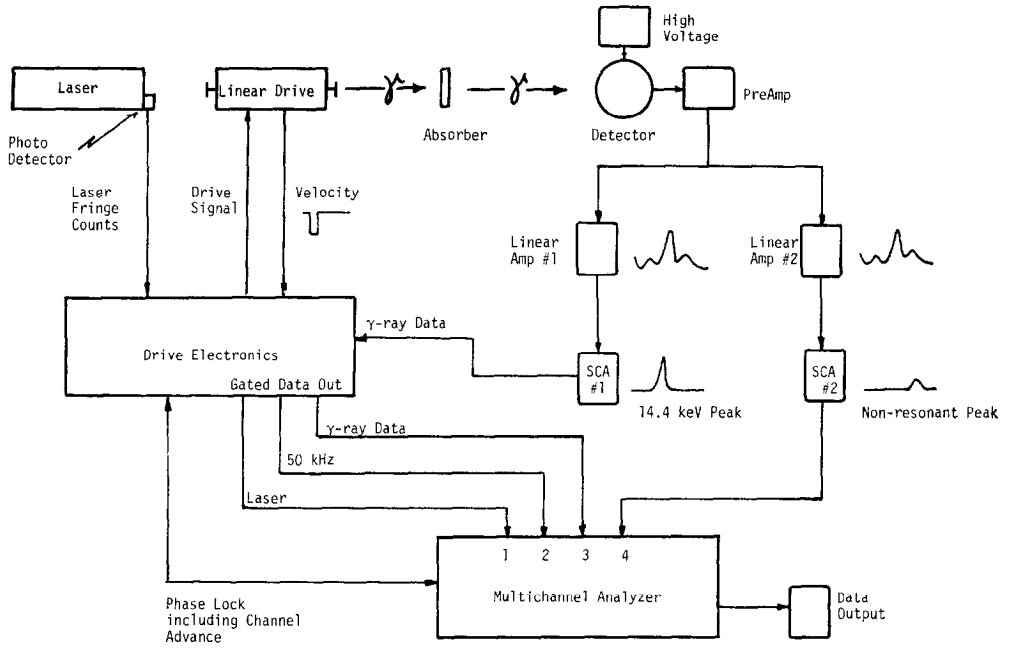

FIG. 1. Schematic of Mössbauer spectrometer configuration for constant velocity operation.

In this investigation we have used *in situ*, constant velocity, Mössbauer effect measurements to follow the rate of conversion of iron metal to iron carbide during the Fischer–Tropsch synthesis reaction. Simultaneous kinetic measurements show a close correlation between carbide formation and reaction rate and selectivity demonstrating, for the first time, the utility of the Mössbauer effect for following transients in catalytic reactions.

EXPERIMENTAL METHODS

Mössbauer spectroscopy. Constant acceleration Mössbauer spectra are obtained with the conventional electromechanical system and stainless-steel absorber cell described previously (*1*). The equipment configuration for our constant velocity Mössbauer effect measurements is shown schematically in Fig. 1. Transmitted γ-rays are detected by the proportional counter. The preamplified signal is split and routed to two separate linear amplifier/SCA combinations; one selecting the 14.4-keV resonance γ-ray pulses, the other selecting pulses in a nonresonant energy region. Rather than using the familiar sawtooth waveform of a constant acceleration drive mode, the Austin Sciences Associates drive electronics produces an asymmetric square-wave signal inducing constant velocity over 80% of the drive motion. In these experiments the velocity was given a slight slope so that it varied by about 0.2 mm/sec. This ensures that slight changes in operating conditions do not shift the peak being studied out of the range of the velocity window. A helium–neon laser interferometer monitors the absolute velocity of the drive rod. The drive electronics gate off the laser fringe counts, 50-kHz timing counts, and the 14.4-keV γ-ray counts during the periodic retrace of the drive motion. These gated signals and the nonresonant count signal are routed to four separate sections of the multichannel analyzer (Nuclear Data Model 2200) memory via a Nuclear Data four input multiscaler. The nonresonant measurement is included

as a check to be sure that changes in resonant count rate are due to chemical change in the catalyst absorber and not due to electronic fluctuations. In these experiments the dwell time per channel was 160 sec, but other times can be selected. The actual dwell time per channel, as measured by the 50-kHz timing counts, varied slightly. Data reported here as counts per channel are normalized for this variation and, therefore, also represent relative count rate.

In order to use this approach to follow the carbiding of iron we have taken advantage of the fact that the right peak of the six-line iron metal spectrum has no overlap with any of the iron carbide peaks since the internal magnetic fields are smaller for the carbides than for the metal. Thus by recording the transmission at the maximum dip of that peak for Fe^0, we can follow the loss of iron metal quantitatively (within a slight error due to small changes in linewidth or position). Full spectra taken after transient runs confirm previous carbide assignments (*2*).

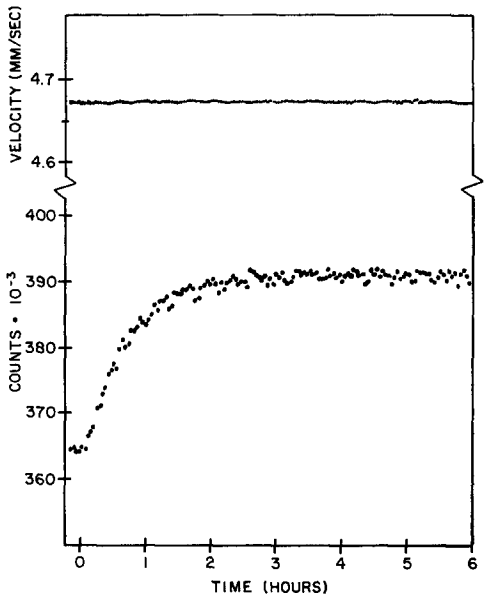

FIG. 2. Constant velocity Mössbauer effect data for the iron to iron–carbide transformation during Fischer–Tropsch synthesis over $10Fe/SiO_2$.

Chemical kinetics. During Fischer–Tropsch synthesis reactions, a Hewlett–Packard Model 5834A reporting gas chromatograph (gc) is used to analyze carbon dioxide and hydrocarbon products in the effluent gas from the Mössbauer cell. This analytical device combines microprocessor control, temperature programming of the Chromosorb 102 column, and digital thermal conductivity detection to give processed data, good separation, and high accuracy ($\pm 3\%$) and sensitivity (~ 5 ppm CH_4) for carbon dioxide and C_1 through C_5 paraffins and olefins. Hydrogen and carbon monoxide peaks are not well resolved, partly because of use of He as a carrier gas. Water is removed prior to sampling with a packed bed of drierite because it overlaps the C_3 peaks. Absolute calibration of the gc is obtained before each run by averaging analyses of three samples of a Certified Standard calibration gas mixture (0.47 He, 0.47 CO, 0.02 CH_4, 0.006 C_2H_6, 0.003 C_2H_4, 0.004 C_3H_8, 0.002 C_3H_6, 0.002 nC_4H_{10}, 0.002 nC_5H_{12} by volume) prepared by Matheson. Blank runs on the stainless-steel cell with no catalyst wafer show that no hydrocarbons can be detected when 50 cc/min of 3.3 H_2/CO feed gas is passed through the cell at 523°K. Similar blank runs with a feed of calibration gas show that at 523°K the cell walls do not cause a change in product distribution within the experimental error of the analysis.

Carbon monoxide conversions are calculated as the *percentage* of the CO molecules entering the reactor that are detected as hydrocarbon products. Since conversions are typically around 3–4% or less, the Mössbauer cell behaves as a differential reactor, thereby minimizing bulk heat and mass transfer difficulties (*3*), effects due to product inhibition (*4*), and complications due to reverse reactions (*5*). The iron on SiO_2 catalysts are prepared by incipient wetness as described earlier (*1*). The iron

on MgO catalysts are prepared according to the method of Boudart *et al.* (*6*) as discussed in Ref. (2).

RESULTS AND DISCUSSION

Carbide Formation

Figure 2 shows typical constant velocity Mössbauer effect data representing extent of iron carbide formation during Fischer–Tropsch synthesis over a supported iron catalyst. The catalyst in this case is a freshly reduced $10Fe/SiO_2$ sample with intermediate metal particle size ($\sim$7.5 nm). The plot of counts vs time shows dramatically that we can indeed follow the course of the solid phase conversion of iron metal to iron carbide with this technique. Time zero is slightly offset; the first few channels, indicated as negative reaction time, measure the intensity of the positive outer metallic iron peak of the prereduced catalyst at reaction temperature $T = 523°K$ in a flowing helium atmosphere prior to reaction. At time zero, 3.3 H_2/CO synthesis gas is introduced into the cell at 100 cc/min. The immediate increase in counts corresponds to a decrease in the Fe^0 peak intensity as iron is converted to iron carbide. The counts continue to increase monotonically until finally, after about 3 hr of reaction, only the baseline is being counted, indicating that at this point the iron is fully carbided. The absolute average velocity of the Doppler drive, computed for each point from laser interferometer data and plotted above vs time, is indeed constant over the course of the run. The standard deviation of the average velocity of 0.001 mm/sec gives a measure of the small error in the energy modulation. Since the absolute velocity is not corrected for cosine smearing, the average Doppler shift, is slightly smaller in magnitude than the measured Doppler shift. For our source-detector geometry, the average value of the velocity error from the cosing effect is typically much less than 1% of the average velocity (i.e., for this run $|\Delta V| = 0.007$ mm/sec). Nonresonant γ-ray data show no change in count rate vs time, proving that the observed change in count rate for the 14.4-keV transition cannot be attributed to fluctuations in the counting electronics.

Similar runs for different iron catalysts confirm the earlier conclusion from the room temperature constant acceleration spectra (*2*) that carbiding rate is a function of average iron metal particle size. These experiments also show that flushing the reactor with He just prior to cooling is a useful quenching method since subsequent Mössbauer spectra give a fairly accurate measure of the extent of carbiding at a given reaction time.

In order to follow the catalytic consequences of the carbide formation, we focus first on the lower curve in Fig. 3 which compares the Mössbauer constant velocity measurement of carbiding with conversion of carbon monoxide by Fischer–Tropsch synthesis over $10Fe/SiO_2$. This conversion curve, contrary to the others in this paper, includes the CO reacted to CO_2 as well as to hydrocarbons. The CO_2 fraction of the products was constant at about 10%. The Fe particle size for this catalyst was $\sim$10 nm (*1*) and the reaction conditions were the same as those used for Fig. 2. Figure 3 reproduces earlier findings (*7*, *8*) that iron carbide is more active than iron metal and shows, in addition, a close correspondence between the amount of carbide formed and the raction rate. Over the initial 2 hr of reaction, conversion increases slightly faster than carbide formation, but from this point conversion and extent of carbiding increase at almost identical rates. We envision the initial carbiding reaction as requiring dissociative adsorption of CO followed by diffusion of carbon into the iron lattice to form the interstitial iron carbide. Since carbon is laid down at the surface, where the reaction is occurring, one might expect the surface to be more completely carbided than the bulk and that

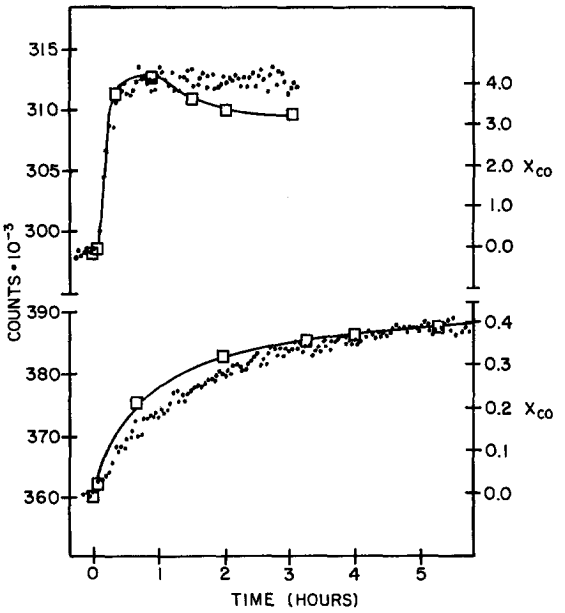

FIG. 3. Percent conversion (solid lines) and extent of carbide formation (points) versus Fischer–Tropsch synthesis reaction time. The upper curve is for 10Fe/MgO. The lower curve is for 10Fe/SiO_2.

the reaction should accelerate faster than total carbide formation. It is remarkable, therefore, that the rate follows the measured bulk carbide formation all the way to completion. We conclude that even at long reaction times surface reconstruction due to iron carbide formation is still occurring. Thus the bulk-phase iron acts as a getter for surface carbon, thereby controlling surface composition and, hence, the active site density of the catalyst.

The upper curve in Fig. 3 for <4-nm particles of Fe on MgO supports the conclusions drawn above. The small particles carbide faster. The rates of carbiding and reaction at the surface are even more closely matched than for the lower curve because of the relatively short diffusion path to the centers of the particles. The reaction conditions for Fe/MgO were identical to those used for Fe/SiO_2 except that a larger sample and slower flow rate (ca. 0.45 g and 50 cc/min, respectively) were employed to increase conversion to the 4% level. Catalyst activity, as measured by conversion, reaches a maximum in the same 30- to 40-min time period required for complete carbiding but then declines. This deactivation cannot be due to sintering, since X-ray diffraction revealed no significant change in particle size for the short reaction times studied nor, for that matter, for various treatments at temperatures up to 723°K. Based on the results of Dwyer and Somorjai (*9*) and other work in this laboratory, the most likely cause of activity loss is deposition of a carbon overlayer on the active iron carbide surface.

Further evidence that bulk iron carbide formation is important for Fischer–Tropsch reactions over iron catalysts is provided by additional transient kinetic studies completed in this laboratory (*10*). For FeNi and FeRu on silica catalysts, systems which do not form bulk carbides during reaction (*2*, *11*), the shapes of the conversion vs time curves contrast sharply with those for unalloyed Fe on silica. The alloy catalysts show a rapid increase in activity at reaction

TABLE 1

Turnover Numbers for Silica-Supported Iron Catalysts at 523°K

Catalyst–source	$N_{CH_4} \times 10^3$ (molecules/site-sec)		$N_{CO} \times 10^3$ (molecules/site-sec)	
	a	*b*	*a*	*b*
$10Fe/SiO_2$– Mössbauer reactor	26	0.5	48	0.9
$10Fe/SiO_2$– conventional reactor	16	0.8	26	1.3
$5Fe/SiO_2$– Vannice (*13*)	15	—	—	—

[a] Based on H_2 chemisorption on fresh, reduced sample.
[b] Based on particle size from X-ray line broadening of the used sample.

time less than 5 min, followed by a decay in rate with time. This behavior differs markedly from the long-term transient response shown here for supported iron.

The stainless-steel *in situ* Mössbauer cell was not originally designed for simultaneous kinetic measurements. In particular, although the inlet gas passes directly over the catalyst wafer, the flow configuration does not guarantee that all the reactant gas contacts the catalyst. To check the validity of the measured rates we compare, in Table 1, turnover numbers at 523°K and 3.3 H_2/CO for silica-supported iron catalysts obtained from the *in situ* Mössbauer cell, from a conventional differential kinetics reactor in this laboratory (*12*), and from Vannice's data (*13*). The table shows intra- and interlaboratory consistency for turnover numbers based on hydrogen chemisorption on fresh, reduced samples but reveals a large difference between turnover numbers based on surface sites determined from chemisorption and those based on surface sites determined from X-ray line broadening. Hydrogen uptakes per gram of supported iron catalyst were very low in every case, indicating that dispersions were less than 1% for both Vannice's catalyst (~0.6%) and ours (~0.2%). Furthermore, Vannice's methane turnover numbers vary by almost an order of magnitude depending on whether dispersion is based on H_2 or CO uptakes. Although it appears that further work is needed to provide a reliable measure of the number of iron surface sites, we conclude on the basis of the (a) columns in Table 1 that rate measurements from the Mössbauer cell are of the right magnitude.

Selectivities from the Mössbauer cell, illustrated in Fig. 4, also show relatively good agreement with those obtained from conventional kinetic studies. Conditions for comparison were chosen such that con-

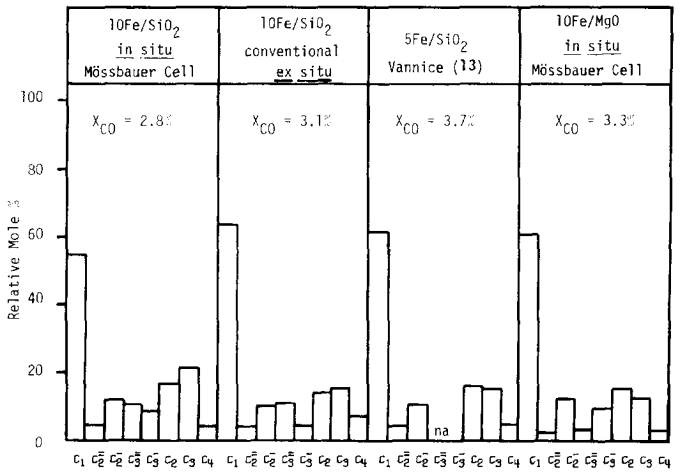

FIG. 4. Selectivities on a CO_2-free basis for supported iron catalysts. C_1, Methane; $C_2^=$, ethylene; C_2^-, ethane; $C_3^=$, propylene; C_3^-, propane; C_2, total C_2s; C_3, total C_3s; C_4, total C_4s.

versions were approximately the same, since selectivity can be a function of total conversion (*10*, *14*). The 10Fe/SiO_2 catalyst studied in the Mössbauer cell reactor produced slightly less methane and correspondingly more C_3s than those run *ex situ*. The selectivities are reported in Fig. 4 on a CO_2-free basis, and so do not show that the iron on magnesia catalyst produced excessive amounts (~50% of products) of carbon dioxide. The rate of CO_2 production was not strongly dependent on the degree of carbiding of the iron and, thus, shows that CO_2 is not simply a product of the carbiding reaction.

Examination of shifts in selectivity as the catalyst becomes carbided reveals, in accord with the results of Amelse *et al.* (*15*), that the most significant changes occur for saturated vs unsaturated hydrocarbons and for relative amounts of higher hydrocarbons. These changes, represented as paraffin/olefin ratio and C_2/C_1 ratio, along with conversion and extent of bulk carbiding, are shown vs time in Fig. 5 for a 10Fe/SiO_2 catalyst with intermediate (~7.5-nm) metal particle size. The plot shows that as carbiding of the iron proceeds, a relatively greater amount of saturated vs unsaturated hydrocarbons is produced. It is not clear whether this shift is caused directly by changes in the catalyst surface or indirectly by increased conversion. The paraffin/olefin ratio is typically particularly sensitive to conversion, with olefinic hydrocarbons being progressively harder to maintain as conversion is increased (*10*, *14*). Following complete carbiding, after about 2 hr of reaction, slight catalyst deactivation, as reflected by a slow decrease in conversion, is accompanied by a continual, but slow, increase in the paraffin/olefin ratio.

The increased favoring of chain growth reactions with time on stream, represented in Fig. 5 as C_2/C_1 ratio, appears to be directly related to the reconstruction in the catalyst surface which accompanies

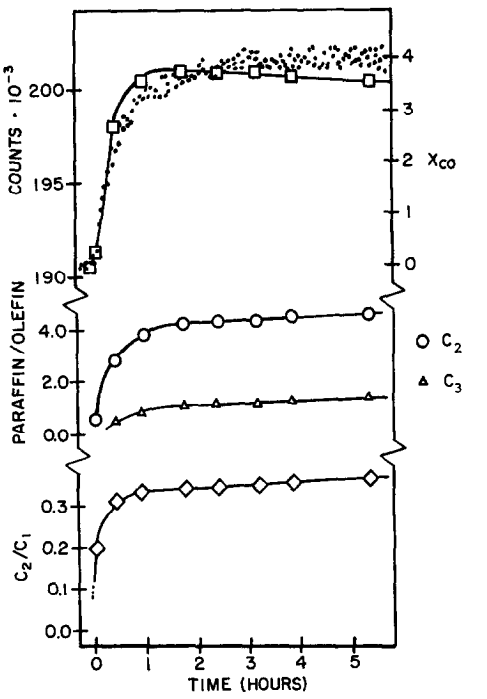

FIG. 5. Selectivities, percentage conversion (upper solid line), and extent of carbide formation versus Fischer–Tropsch synthesis reaction time for 10Fe/SiO_2.

carbide formation. The results of Dwyer and Somorjai (*9*), showing that polycrystalline iron foil is predominantly a methanation catalyst which poisons rapidly by the deposition of multilayers of surface carbon, support our observation that the original iron-rich surface is methane selective. We note that in comparisons between the catalytic behavior of iron particles and iron foils, one should account for differences in the time it takes to form the saturated bulk carbide and differences in the extent of carbon overlayer deposition.

Reversibility in Hydrogen

Further insight into Fischer–Tropsch chemistry can be obtained through application of constant velocity Mössbauer spectroscopy to the reverse of the carbiding reaction, the hydrogenation of the carbide. The fully carbided 10Fe/MgO catalyst was

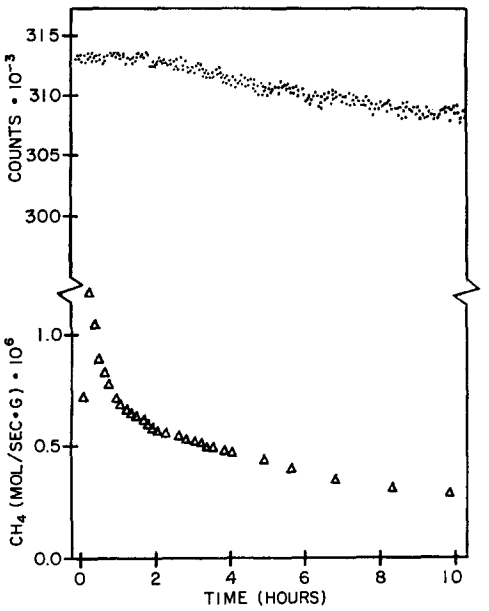

FIG. 6. Hydrogenation of carbide 10Fe/MgO at 523°K. The upper curve is counts in the highest velocity Fe^0 Mössbauer line, the lower curve is the rate of methane production; both as a function of time of exposure to H_2.

hydrogenated in 50 cc/min of hydrogen at 523°K for 10 hr. Extent of hydrogenation was monitored through the intensity increase of the highest velocity Fe^0 peak, and gas-phase reaction products were measured with gas chromatography. The corresponding plot of the γ-ray counts vs time (Fig. 6) reveals that the hydrogenation reaction is extremely slow relative to the carbiding reaction. Even after 10 hr only about 30% of the iron carbide had been hydrogenated to metallic iron. This is interesting in light of kinetic studies which show, in every case, that the initial, low catalytic activity characteristic of iron metal catalysts is reestablished after only a few hours of hydrogenation at 523°K. Thus, the data support a model in which the surface layers of the carbided catalyst are quickly converted to metallic iron, leaving a relatively pure core of bulk carbide intact. The slow step in carbide reduction appears to be movement of carbon across the bulk/surface interface.

Methane was the only hydrocarbon product detected in the gas phase during hydrogenation. As shown in Fig. 6, the rate of methane formation goes through a sharp maximum near 10–12 min and then decreases quickly until at about 2 hr the decrease in methane production is very slow and tracks the increase in the Fe^0 Mössbauer peak intensity. This general form of the methane production curve has been observed previously (*16*) for hydrogenation of ϵ-carbide in a fused iron catalyst. Even at the highest methanation rate observed, the rate is still a factor of four less than the rate of methanation at the end of the 6-hr Fischer–Tropsch synthesis run. This result suggests either that direct hydrogenation of surface carbidic carbon is not responsible for production of a majority of methane in the synthesis reaction, or that the reaction is structure sensitive and the most active sites are replenished by dissociative adsorption of CO. This conclusion is in good agreement with the findings of Matsumoto and Bennett (*17*) that carbidic carbon is relatively inactive compared to the active surface carbon formed in the presence of both CO and H_2.

CONCLUSIONS

We have shown with *in situ* spectroscopic and kinetic measurements that formation of iron carbide during reaction is intimately involved in the development of maximum activity for Fischer–Tropsch synthesis over supported iron catalysts. Similar conclusions have been drawn independently by Matsumoto and Bennett in transient kinetic studies of fused iron catalysts (*17*). Chemisorption studies on iron single crystals (*18*, *19*) and foils (*20*, 21) show that CO adsorbs dissociately at room temperature, making this step a possible starting point for carbide formation at reaction conditions, but a variety of intermediates (*17*) can account for the close association of carbide build up and hydrocarbon synthesis activity. It is evident from the well-

documented but different explanations of Fischer–Tropsch activity now appearing [e.g. (*22*, *23*)] that the important catalytic chemistry is likely to depend on reaction conditions and catalyst. Specific conclusions drawn from this work on the iron–carbon system include:

(1) The extent of iron carbide formation tracks the increase in catalyst activity, showing that the presence of iron carbide is important for this reaction and that carbon incorporation by the iron bulk controls the concentration of active surface sites.

(2) The catalyst becomes more selective to higher hydrocarbons as the iron carbides. The increase in paraffin/olefin ratio may be caused by the increase in conversion rather than the change in the chemical nature of iron.

(3) Hydrogenation of bulk iron carbide occurs at a much slower rate than either corresponding carbiding or hydrocarbon synthesis during the Fischer–Tropsch reaction. Thus, if direct hydrogenation of a surface carbidic carbon is important in the reaction sequence, it must occur on a relatively small number of special sites.

(4) Hydrogenation of surface and bulk iron carbide produces only methane.

ACKNOWLEDGMENTS

We thank the National Science Foundation for support of this work through Grants ENG76-020853 and DMR76-00889A1, and D. P. Aschenbeck for assistance in achieving *in situ* Mössbauer analysis.

REFERENCES

1. Raupp, G. B., and Delgass, W. N., *J. Catal.* **58**, 337 (1979).
2. Raupp, G. B., and Delgass, W. N., *J. Catal.* **58**, 348 (1979).
3. Pichler, H., and Schulz, H., *Chem. Eng. Tech.* **42**, 1162 (1970).
4. Pichler, H., and Hector, A., "Kirk-Othmer Encyclopedia Chem. Tech. IV," 446 (1964).
5. Nefedov, B. K., and Eidus, Ya. T., *Russian Chem. Rev.* **34**, 272 (1965).
6. Boudart, M., Delbouille, A., Dumesic, J. A., Khammouma, S., and Topsøe, H., *J. Catal.* **37**, 486 (1975).
7. Anderson, R. B., *in* "Catalysis" (P. H. Emmett, Ed.), Vol. IV, pp. 29, 257. Reinhold, New York, 1956.
8. Hofer, L. J. E., *in* "Catalysis" (P. H. Emmett, Ed.), Vol. IV, p. 373. Reinhold, New York, 1956.
9. Dwyer, D. J., and Somorjai, G. A., *J. Catal.* **52**, 291 (1978).
10. Lauderback, L. L., Kostka, W. D., and Delgass, W. N., to be published.
11. Aschenbeck, D. P., Forunato, F. A., and Delgass, W. N., to be published.
12. Kostka, W. D., and Delgass, W. N., to be published.
13. Vannice, M. A., *J. Catal.* **50**, 228 (1977).
14. King, D., *J, Cal.* **51**, 386 (1978).
15. Amelse, J. A., Butt, J. B., and Schwartz, L. H., *J. Phys. Chem.* **82**, 558 (1978).
16. Rozovskii, A. Y., Savel'ev, V. Ya.. Kagan, Yu. B., and Stytsenko, V. D., *Kinet. Katal.* **9**, 452 (1968).
17. Matsumoto, H., and Bennett, C. O., *J. Catal.* **53**, 331 (1978).
18. Yoshida, K., and Somorjai, G. A., *Surface Sci.* **75**, 46 (1978).
19. Brundle, C. R., *IBM J. Res. Dev.* **22**, 235 (1978).
20. Barber, M., Vickerman, J., and Wohlstenholme, J., *Surface Sci.* **68**, 130 (1977).
21. Fleisch, T., Winograd, N., and Delgass, W. N., unpublished results.
22. Ponec, V., *Catal. Rev.-Sci. Eng.* **18**, 151 (1978).
23 Biloen, P., Helle, J. N., and Sachtler, W. M. H., *J. Catal.* **58**, 74 (1979).